Australian Government

Geoscience Australia

GEOPHYSICAL SURVEY DATA AND METADATA, BILLABONG CREEK, NEW SOUTH WALES

Adrian Fisher and Ross Brodie

This report was produced by Geoscience Australia (GA) for the Bureau of Rural Sciences (BRS) project: Salinity mapping – Geophysics. The report was submitted to BRS on 12/6/2008.

Disclaimer

Geoscience Australia has tried to make the information in this product as accurate as possible. However, it does not guarantee that the information is totally accurate or complete. Therefore, you should not solely rely on this information when making a commercial decision.

Executive summary

This report describes airborne geophysical and gravity data for the Billabong Creek area, near Albury in southern New South Wales. The airborne geophysical surveys were conducted to provide information on land management issues. The first section of the report describes different datasets that have been acquired and processed (processed data), and the second section lists the different products that have been derived from those datasets (derivative data). The data described are presented on the DVD that accompanies this report.

The section describing processed data includes descriptions of the Billabong Creek airborne electromagnetic (AEM) survey; the Billabong Creek airborne magnetic, gamma-ray and elevation (MAGSPEC) survey; and, an extract of the Australian National Gravity Database (GRAVITY). While the processed data should be considered the fundamental geophysical data they have limited use to those without specialised geophysical knowledge and computer software. The derivative products have been specially designed to enable geologically meaningful information to be extracted from them more easily than from the fundamental data. However, they should only be considered depictions of the data, and the methods used in their generation instil their own biases.

The main derivative products from the AEM survey are conductivity - depth slices and sections, as well as conductance grids and interpreted basement surfaces. Products derived from the MAGSPEC survey include images of the magnetic and gamma-ray signatures, as well as a digital elevation model. An image processed depiction of the gravity data is also presented. All image files are stored in the JPEG (.jpg) format, which can be viewed by most computers. They also have associated world files (.jgw) that allow the images to be displayed in a geographic information system (GIS). Some ESRI shapefiles were also produced to help visualise some aspects of the data, which can be displayed in the ESRI ArcGIS software package.

Contents

Executive summary **iii**

List of figures **v**

List of tables **v**

1. Introduction **1**

2. Processed data **1**

2.1 AEM survey 2

2.2 MAGSPEC survey 5

2.3 Gravity surveys 8

3. Derivative products **12**

3.1 Glossary of image enhancement techniques 12

3.2 AEM products 13
3.2.1 Previous AEM products 13
3.2.2 Geoscience Australia layered earth inversion (GA LEI) 14

3.3 Magnetic products 20

3.4 Gamma-ray products 22

3.5 DEM products 24

3.6 Gravity products 25
3.6.1 Enhanced gravity image 25
3.6.2 Gravity station shapefile 25

Appendix A – Technical specifications of the AEM survey and system **29**

Appendix B – Technical specifications of the MAGSPEC survey and system **30**

Appendix C – Airborne geophysical survey boundary coordinates **31**

Appendix D – Technical specifications of map projections **32**

Appendix E – Data stored on the accompanying DVD **33**

List of figures

Figure 1 Location of the AEM and MAGSPEC surveys, and the gravity data extract. 1

Figure 2 1-dimensional inversion with a vertically smooth model. Independent 1-dimensional models are calculated for each sample point along each flight line. The thickness of each layer (t_n) is fixed, and the conductivity (σ_n) is allowed to vary between layers, shown by the changing colours. Each 1-dimensional model assumes that the conductivity of each layer is laterally constant. Note that the diagram is not to scale and in reality sample points are ~12 m apart. 14

Figure 3 Creating flight-line conductivity-depth sections from the modelled conductivity predictions. The sample points are first interpolated horizontally onto a line of best fit (a). The inversion results (b) are then interpolated vertically (c) into an evenly spaced grid. Note that the sample points are spaced every ~12 m along the line. A horizontal five point median filter is applied to each layer. 17

Figure 4 Creating conductivity-depth slices from the modelled conductivity predictions. 18

Figure 5 Conductivity-depth slice (pseudocolour linear colour stretch with an E-W gradient enhancement) for 0-5 m depth from the GA LEI of the Billabong Creek AEM data. 19

Figure 6 Enhanced image of TMI-RTP from the Billabong Creek MAGSPEC survey data. 21

Figure 7 Enhanced ternary gamma-ray image from the Billabong Creek MAGSPEC survey data. 23

Figure 8 Enhanced DEM image from the Billabong Creek MAGSPEC survey data. 24

Figure 9 Enhanced image of Bouguer gravity anomaly data and the location of gravity survey stations (red dots) for the Billabong Creek area. 26

List of tables

Table 1 Details of the 15 windows used in the processing of the Billabong Creek AEM survey data. 4

Table 2 Energy limits of the windows used in processing of the gamma-ray data. 7

Table 3 Gravity surveys in the Billabong Creek region of NSW. The first four digits of each survey's ID are derived from the year the survey was undertaken. 11

1. Introduction

This report describes the data and metadata for airborne geophysical and gravity surveys carried out in the Billabong Creek area, near Albury in southern New South Wales (Figure 1). The report has two main sections: the first section describes the different datasets that have been acquired and processed; the second section lists the different products that have been derived from those datasets. Technical details have been included in the appendices, which also contain a list detailing the digital files that accompany the report. The processed data described in the first section should only be used by experienced users of software designed to work with geophysical data. The derivative products described in the second section have been designed to enable geologically meaningful information to be extracted from them more easily than from the fundamental data, however, they should only be considered as depictions of the data, and not the data itself.

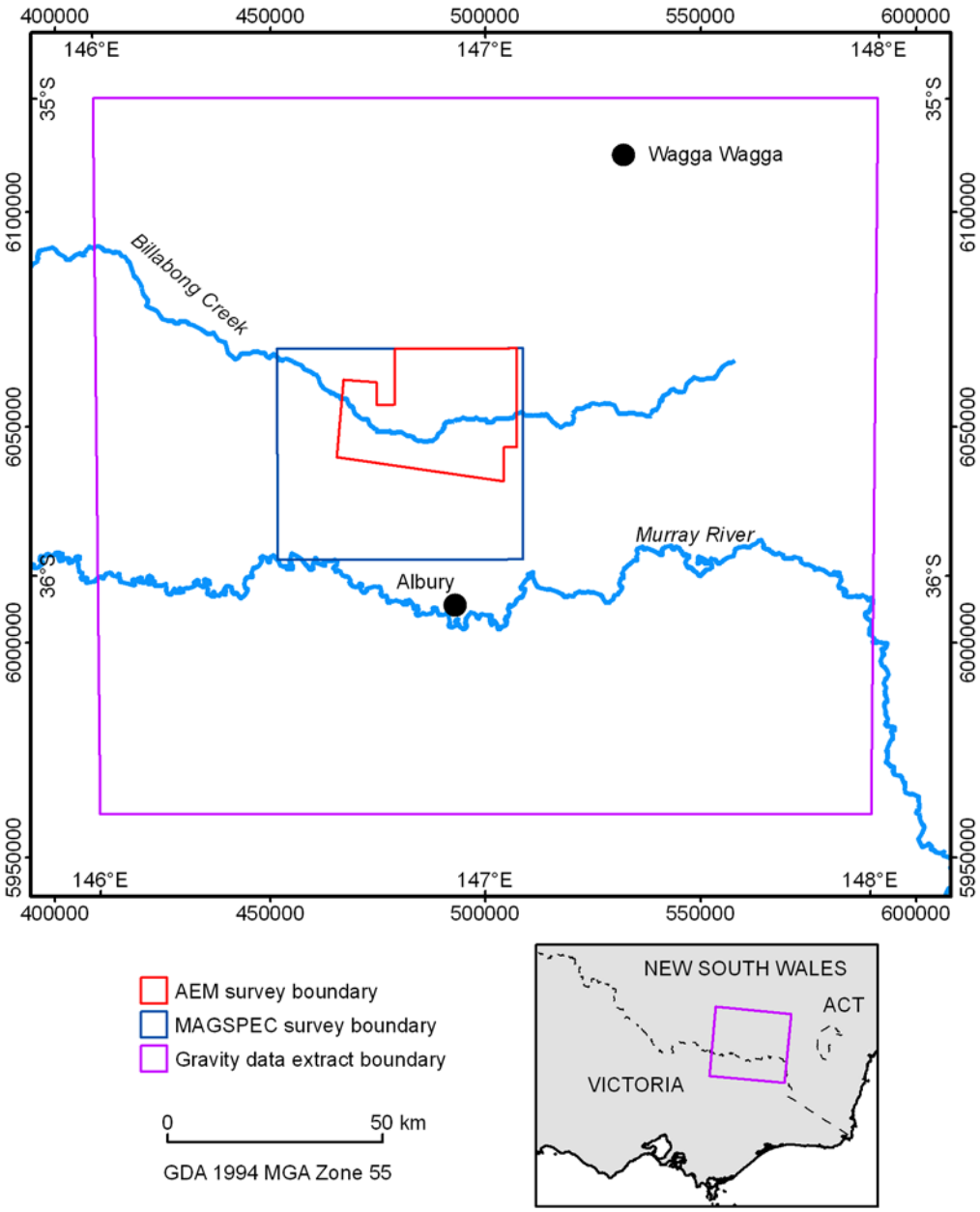

Figure 1 Location of the AEM and MAGSPEC surveys, and the gravity data extract.

2. Processed data

This report considers three different geophysical datasets that have been acquired and processed for the Billabong Creek region of NSW: an airborne electromagnetic (AEM) survey; an airborne magnetic, gamma-ray and elevation (MAGSPEC) survey; and, an extract of the Australian National Gravity Database (GRAVITY).

The airborne surveys were commissioned by the Murray Darling Basin Commission (MDBC) during 2001. Fugro Airborne Surveys Pty Ltd (Fugro) was contracted to acquire and process the AEM survey utilising the TEMPEST time domain airborne electromagnetic system described by Lane *et al.* (2000). Kevron Geophysics Pty Ltd (Kevron) was contracted to acquire and process the MAGSPEC survey utilising an industry standard system (Horsfall, 1997). Both surveys were project managed and contracted through the Bureau of Rural Science (BRS), while Geoscience Australia managed and quality controlled the work of Kevron and Fugro.

2.1 AEM survey

Summary
The AEM survey data was acquired by Fugro between the 31st of August and the 19th of September, 2001. The system operated through transmitting a primary electromagnetic field from a loop attached to a fixed-wing aircraft, and measuring the electromagnetic response of the ground via receiver coils located in a towed bird. The raw measurements were then processed to give the final data, which is in a point located (or line) format.

Survey specifications
The survey was flown along east-west flight lines, spaced 200 m apart, for a total of 5,522 line kilometres. Further technical details of the survey and system are included in Appendix A, summarised from the acquisition and processing report compiled by Fugro (Owers *et. al.*, 2002).

Data format
The AEM survey data are stored in a point located (or line) format, in ASCII (.dat) files formatted with space-delimited columns. Each record represents one sample along a flight line. A comprehensive header file (.hdr) is associated with the ASCII file, which describes the data and the numeric format of each column in the file.

Data extent
The following coordinates describe the geographic extent (bounding box) of the AEM survey data: 35.529^{o}S to 35.807^{o}S latitude and 146.618^{o}E to 147.081^{o}E longitude. The specific boundary of the survey is an irregular polygon (Figure 1), the details of which are given in Appendix C.

Scale and resolution
The fundamental resolution of airborne geophysical measurements is most usually quoted as the “footprint” of the system. The footprint is defined as the area upon the earth from which 90% of the measured response originates. The size of the footprint is a function of the measurement and processing system characteristics and the physics of the quantities being measured. For the Billabong Creek airborne electromagnetic measurements, it is estimated that the footprint has a 200 m radius. The data resolution, however, is a function of the

sampling density along the survey lines and the spacing between survey lines (see Appendix A). While the data are digital and can be viewed at any scale, it is recommended that data with 200 m flight line spacing be presented at 1:50 000 scale.

Positional accuracy
Positioning was via post-processed differential GPS methods. Horizontal positional accuracy of the data is approximately 1 metre (standard deviation). Vertical accuracy of the derived digital elevation model is approximately 2 metres (standard deviation).

Attribute accuracy
The data have been acquired and processed to a standard of best practice as of the year 2001. More sophisticated processing algorithms may be applied to these data should they become available.

Datum and projection
The datum used was the Geocentric Datum of Australia 1994 (GDA94). Point located data are attributed with both geodetic (latitude and longitude) and projected coordinates (eastings and northings). Technical details of the projection used (Map Grid of Australia, Zone 55) are given in Appendix D.

Lineage
The following steps were used in processing the AEM survey data, and have been summarised from the acquisition and processing report compiled by Fugro (Owers *et. al.*, 2002).

1. High altitude pre and post flight calibration data were used to characterise the system response in the absence of any ground response.
2. Routines to suppress spheric noise, powerline noise, VLF noise and coil motion noise were applied to data from survey lines.
3. A three-second wide cosine-tapered stacking filter was then applied to stack the data. Output from the stacking filter was drawn at 0.2-second intervals.
4. The survey line stacked data were deconvolved using the interpolated high altitude reference waveform. The effect of currents in the transmitter loop and airframe ("primary") were then removed.
5. The primary field at the receiver was then estimated and subtracted from the deconvolved data, leaving a "pure" ground response.
6. The position of the receiver relative to the transmitter was then estimated.
7. The deconvolved ground response data were then transformed to B-field response for a perfect 100% duty cycle square wave with a 1A peak to peak step.
8. The evenly spaced samples were binned into 15 windows as specified in Table 1. The output from this step is the "non height- pitch- roll- and geometry-corrected window data" (non HPRG data). Processing steps 1-6 yielded monitor values such as powerline, spherics, VLF and low frequency monitor channels, as well as the "geometric factor" and transmitter to receiver separation values.
9. The output from step 8 was then used to compute "height-pitch- roll- and geometry-corrected window data" (HPRG data) via the method of Green (1998). This accounts for variations in the aircraft's height, pitch and roll as well as the transmitter-receiver geometry. The HPRG data were computed to yield the response that would be expected if all observations had been made with constant aircraft height, attitude and transmitter-receiver geometry.

Availability

The final point located data for the Billabong Creek TEMPEST AEM survey (GA Project # 904) are stored on the data DVD that accompanies this report. It is also available on a CD-ROM from the Geoscience Australia sales centre. The CD-ROM is distributed for a nominal cost of $99. Details of the data are available in the online 'Products Database' by searching for Billabong Creek or GeoCat number 65385. Geoscience Australia also intends to make the data available for free download when this becomes possible.

Table 1 Details of the 15 windows used in the processing of the Billabong Creek AEM survey data.

Window #	Start sample	End sample	No of samples	Start time (s)	End time (s)	Centre time (s)	Centre time (ms)
1	1	2	2	0.000007	0.000020	0.000013	0.013
2	3	4	2	0.000033	0.000047	0.000040	0.040
3	5	6	2	0.000060	0.000073	0.000067	0.067
4	7	10	4	0.000087	0.000127	0.000107	0.107
5	11	16	6	0.000140	0.000207	0.000173	0.173
6	17	26	10	0.000220	0.000340	0.000280	0.280
7	27	42	16	0.000353	0.000553	0.000453	0.453
8	43	66	24	0.000567	0.000873	0.000720	0.720
9	67	102	36	0.000887	0.001353	0.001120	1.120
10	103	158	56	0.001367	0.002100	0.001733	1.733
11	159	246	88	0.002113	0.003273	0.002693	2.693
12	247	384	138	0.003287	0.005113	0.004200	4.200
13	385	600	216	0.005127	0.007993	0.006560	6.560
14	601	930	330	0.008007	0.012393	0.010200	10.200
15	931	1500	570	0.012407	0.019993	0.016200	16.200

2.2 MAGSPEC survey

Summary

The MAGSPEC survey was acquired by Kevron between the 23rd of May and the 12th of July 2001. The aircraft was fitted with a horizontal gradiometer system to measure magnetic anomalies, and a downward looking gamma-ray spectrometer that measured the naturally occurring gamma rays emanating from radioactive materials at the earth's surface. Ground elevation was also determined from the survey data, by subtracting radar altimeter measurements of the aircraft's height above the ground, from GPS measurement of its height above sea level. The final processed data are in point located (or line) format, and have also been converted to grids, which are easier to view. However, to display the data best in map view, it is best to work with software designed to image geophysical data.

Survey specifications

The survey was flown along east-west flight lines, spaced 100 m apart, and north-south tie lines spaced 1000 m apart, for a total of 34 178 line kilometres. Further technical details of the survey and system are included in Appendix B, summarised from the acquisition and processing report compiled by Kevron Geophysics (2001).

Data format

The MAGSPEC survey data are stored as point located (or line) data, in ASCII (.dat) files formatted with space-delimited columns. Each record represents one sample along a flight line. A comprehensive descriptive file (.README) is associated with the ASCII file, which describes the data format for each column. The components of the processed MAGSPEC survey data that were gridded are stored in binary files as ERMapper single band IEEE4Byte Real data types. A comprehensive header (.ers) file is associated with each grid file, which describes the data and the geographic positioning of the grid.

Data extent

The following coordinates describe the geographic extent of the MAGSPEC survey data: 35.529°S to 35.971°S latitude and 146.465°E to 147.097°E longitude (Figure 1).

Scale and resolution

The fundamental resolution of airborne geophysical measurements is most usually quoted as the "footprint" of the system. The footprint is defined as the area upon the earth from which 90% of the measured response originates. The size of the footprint is a function of the measurement and processing system characteristics and the physics of the quantities being measured. The footprints of the various components of the MAGSPEC survey have been estimated as:

- Magnetic NA (depends on anomaly source depth)
- Gamma-ray ~360 metre radius
- Elevation ~10 metre radius

The data resolution of the point located data, however, is a function of the sampling density along the survey lines and the spacing between survey lines (see Appendix B). Data resolution of the gridded data is determined by the grid cell size, which for the MAGSPEC survey data is 20 m (1/5 of the flight line spacing). While the data are digital and can be viewed at any scale, it is recommended that data with 100 m flight line spacing be presented at 1:25 000 scale.

Positional accuracy
Positioning was via post-processed differential GPS methods. Horizontal positional accuracy of the data is approximately 1 metre (standard deviation). Vertical accuracy of the derived digital elevation model is approximately 2 metres (standard deviation).

Attribute accuracy
The data have been acquired and processed to a standard of best practice as of the year 2001. More sophisticated processing algorithms may be applied to these data should they become available.

Geographic datum and projection
The datum used was the Geocentric Datum of Australia 1994 (GDA94). Point located data are attributed with both geodetic and projected coordinates, while gridded data are stored in the projected coordinate system only. Technical details of the projection used (Map Grid of Australia, Zone 55) are given in Appendix D.

Lineage
The following steps were used in processing the MAGSPEC survey data, and have been summarised from the acquisition and processing report compiled by Kevron Geophysics (2001). Each type of data required different processing; accordingly they are discussed separately below.

Processing steps for the magnetic data were:
1. Manual inspection and editing of profile data to remove any noise spikes or bursts
2. Subtraction of the diurnal variation
3. Subtraction of the International Geomagnetic Reference Field (IGRF model 2000)
4. A mean value of the IGRF total field, updated to 2001.5, was added to the data
5. Tie line levelling
6. Microlevelling
7. Gridding (20 m grid cell size)
8. Calculation of reduction to the pole
9. Calculation of first vertical derivative

Processing steps for the gamma-ray data were:
1. Apply the spectral smoothing using the Noise Adjusted Singular Value Decomposition (NASVD) method described by Hovgaard and Grasty (1997)
2. Apply dead-time correction
3. Apply energy calibration
4. Remove aircraft and cosmic background
5. Remove atmospheric radon background
6. Reduce height data to effective heights at standard temperature and pressure
7. Apply Compton scattering (stripping) correction
8 Extract elemental windows from the 256 channel data using window energy limits listed in Table 2.
9. Apply height attenuation correction
10. Conversion to equivalent elemental concentrations and dose rate using the method described in Grasty and Minty (1995).
11. Tie line levelling
12. Microlevelling
13. Gridding of potassium, uranium, thorium and dose rate (20 m grid cell size)

Table 2 Energy limits of the windows used in processing of the gamma-ray data.

Window	Energy (keV) Lower	Upper
Potassium	1370	1570
Uranium	1660	1860
Thorium	2410	2810
Total count	400	2810

The processing steps for the elevation data as conducted by Kevron were:

1. Apply post-flight differential processing of GPS data
2. Subtract radar altimeter from GPS ellipsoidal height
3. Apply correction for GPS antenna and radar altimeter antenna separation
4. Convert ellipsoidal elevations to Australian Height Datum (geoidal) elevations via subtraction of AUSGEOID N values
5. Tie line levelling
6. Microlevelling
7. Gridding (20 m grid cell size)

Availability

The final point located and gridded data for the Billabong Creek MAGSPEC survey (GA Project # 908) are available as a free download from the Geoscience Australia 'Geophysical Archive Data Delivery System' (www.geoscience.gov.au/gadds).

2.3 Gravity surveys

Summary

The Australian National Gravity Database is a freely available compilation of gravity station measurements taken by Geoscience Australia, state and territory Geological Surveys, private companies, educational institutions and other research organisations. Point located gravity data for the Billabong Creek Region was extracted from the database by using the Geoscience Australia Geophysical Archive Data Delivery System (www.geoscience.gov.au/gadds), and was then gridded. To view the distribution of the point located and gridded data most effectively, it is best to work with software designed to image geophysical data.

Survey specifications

As the Australian National Gravity Database is a compilation of many surveys, the survey specifications used in data acquisition vary. Generally speaking, the database consists of many individual stations where gravity measurements were recorded through the use of various types of gravity meters. The extracted data for the Billabong Creek region consists of 27 different surveys.

Data format

The gravity survey data are stored as point located data, in an ASCII (.dat) file, formatted with space-delimited columns, where each record represents one sample. The details of the projection and datum are included in a separate file (.des) as are information on the format of the geophysical data (.dfn). The data are also accompanied by a document that outlines the metadata for the entire Australian National Gravity Database (.doc). The gridded gravity data are stored in a binary file with ERMapper single band IEEE4Byte Real data type. A comprehensive header (.ers) file is associated with the grid file, which describes the data and the geographic positioning of the grid.

Data extent

The Australian National Gravity Database covers the entire country, however, only a small subsection was extracted. The geographic extent (bounding box) of the extracted data is: 35°S to 36.5^{o}S latitude and 146°E to 148°E longitude (Figure 1).

Scale and resolution

The spacing of the gravity survey stations across the entire Australian National Gravity Database ranges from 10 m to 11 km. The subsection of data extracted for the Billabong Creek region has a spacing of around 10 km. The grided data has a cell size of 2 km, which is one fifth of the average station spacing. The data are digital and can be viewed at any scale, though the 2 km grid cell size works best at the regional scale.

Positional accuracy

The positional accuracy of the gravity survey stations is highly variable depending on the age of the individual surveys that comprise the data set. Prior to 1995 (approximately), data were collected using various techniques to determine position such as: manually scaling from base maps (100's m error); digitising from base maps derived from air photo station plots (100's m error); or, optical surveying methods (metre accuracy). Post 1995 most surveys were acquired using differential GPS with sub metre accuracy. Vertical accuracy is also highly variable, depending on the age of the survey. Prior to the use of differential GPS (centimetre accuracy) station heights were determined by: picking from a topographic map (10's metre error); using barometric techniques (metre errors); or, optical surveying techniques (sub metre accuracy).

The ages of the surveys in the Billabong Creek region, and their approximate positional accuracy, are shown in Table 3.

Attribute accuracy

The accuracy of the gravity data is highly variable depending on the age of the individual surveys that comprise the dataset. Modern surveys use LaCoste Romberg or Scintrex gravity meters which have an accuracy of 0.01 μms^{-2} (micrometres per second squared). Earlier surveys used older quartz spring meters with a lower accuracy (approximately 1.0μms^{-2}). The ages of the surveys in the Billabong Creek region, and their approximate attribute accuracy, are shown in Table 3. This information is also contained within the point located ASCII (.dat) file.

Geographic datum and projection

The datum used was the Geocentric Datum of Australia 1994 (GDA94). Point located data are attributed with both geodetic and projected coordinates, while gridded data are stored in the projected coordinate system only. Technical details of the projection used (Map Grid of Australia, Zone 55) are given in Appendix D.

Lineage

All data within the Australian National Gravity Database have been processed according to the first four steps below. The fifth step was also applied to the downloaded subset of Billabong Creek data to produce the *ER Mapper* Grid.

1. Normal (theoretical) gravity based on the 1980 international gravity formula (Moritz, 1980):

   $G_n = 9780326.7715*((1+0.001931851353(\sin^2\theta)/(SQRT(1-0.0066943800229(\sin^2\theta)))$
   where θ represents degrees of latitude

2. An atmospheric correction (δg_{atm}) was applied to the normal (theoretical) gravity to correct for the gravity effect of the atmosphere. This correction is SUBTRACTED from the theoretical gravity value calculated from the equation above. The atmospheric gravity effect is approximated using the following equation (Wenzel, 1985):

   $\delta g_{atm} = 8.74 – 0.00099*h + 0.0000000356*h2$
   where h = ellipsoid height in metres and the units for atmospheric correction are in micrometres/sec/sec.

3. The free air correction (FAC) is then calculated using the ellipsoid height and a second order approximation equation (Heiskanen and Mortiz, 1969):

   $FAC = (3.08768 – 0.00440\sin^2\phi)*h + 7.2125*10^{-7}*h^2$

   The Free Air Anomaly (FAA) is given by the following equation:

   $FAA= G_{obs} – (G_n - \delta g_{atm}) - FAC$
   where G_{obs} = observed gravity

4. The Bouguer correction is calculated using the closed form equation for the gravity effect of a spherical cap of radius 166.7 km (La Fehr, 1991) based on a spherical Earth with a mean radius of 6,371.0087714 km, height relative to the ellipsoid, and a density of 2.67 t/m3 (for solid earth).

$BC = 2\pi G\rho((1+\mu)*h - \lambda R)$
where:
π is pi;
G is the gravitational constant; = 6.67428 x 10-11 m3kg-1s-2 (Mohr and Taylor 2001);
ρ is density in t/m3 typically 2.67t/m3;
h is the ellipsoid height in metres of the station;
R = (Ro + h) the radius of the earth at the station; and,
Ro is the mean radius of the earth = 6,371.008 771 4 km GRS 80 value from Moritz;
μ & λ are dimensionless coefficients with following definitions:
$\mu = ((1/3)*\eta 2 - \eta)$ where
$\eta = h/R$
$\lambda = (1/3)\{(d + f\delta + \delta 2)[(f - \delta)2 + k]1/2 + p + m*\ln(n/(f - \delta + [(f - \delta)2 + k]1/2)\}$
where:
$d = 3*\cos 2\alpha - 2$;
$f = \cos\alpha$;
$k = \sin 2\alpha$;
$p = -6*\cos 2\alpha \sin(\alpha/2) + 4*\sin 3(\alpha/2)$;
$\delta = Ro/R$;
$m = -3*\sin 2\alpha \cos\alpha = -3*k*f$;
$n = 2*[\sin(\alpha/2) - \sin 2(\alpha/2)]$; and,
$\alpha = S/Ro$, with S = Bullard B Surface radius = 166.735 km.

The Bouguer Anomaly (BA) in μms^{-2} is given by the equation:

BA = FAA - BC

5. Using the variable density gridding function within the *Intrepid* software package (version 4.1), the data from step 4 (Bouguer gravity anomaly) were gridded to an *ER Mapper* raster dataset with a 2 km grid cell size.

Availability
Point located data from the Australian National Gravity Database can be downloaded free of charge from the Geoscience Australia Geophysical Archive Data Delivery System (www.geoscience.gov.au/gadds). The section extracted over the Billabong Creek region is also available on the DVD that accompanies this report.

Table 3 Gravity surveys in the Billabong Creek region of NSW. The first four digits of each survey's ID are derived from the year the survey was undertaken.

Survey ID	Survey name	Number of stations	Horizontal accuracy (m)	Vertical accuracy (m ahd)	Gravity accuracy (μms^{-2})
195099	Cambridge Pendulum Isogals	1	500	1.5	6
195103	Melbourne-Albury-Wagga Wagga, Grav	25	100	0.3	0.1
195607	Wangaratta-Mt Beauty-Power Station Grav	4	200	5	0.1
195903	Melbourne-Forbes-Sydney-Canberra, Grav	13	100	1.52	0.1
196104	East Victoria Grav	62	100	5	0.5
196401	North East Victoria Grav	7	250	5	0.1
196491	Isogal Grav, Australia	1	100	5	0.1
196541	Wagga Wagga-Newcastle Grav	21	540	0.3	0.15
196591	Central, Eastern Australia Calibration Line	2	100	5	0.1
196604	Southern NSW Region Grav	5	100	5	0.1
196606	Helicopter Grav Training Survey ACT, Southern NSW	19	100	3.35	1
196793	Isogal Grav by aircraft Australia	1	100	5	0.1
196933	Jerilderie Detailed Grav	6	96.44	0.3	1
197206	Goulburn, Owen River Valleys, Grav	24	50	0.3	0.2
197300	Helicopter Grav SE Australia	250	50	5	0.5
197301	Helicopter Grav SE Australia	12	50	5	0.5
197591	Isogal Follow up Melbourne, Albury, Grav	1	100	5	0.1
197805	Lachlan Structure Grav	2	200	1	0.5
198001	Lachlan Fold Belt Grav Traverses	142	75	0.5	0.2
198090	Isogal Grav Strengthening	1	100	5	0.1
198702	Tumut Seismic Traverse, Grav	4	100	2	0.5
199736	Wadderburn 1:100,000 Infill	323	1	1	0.5
199930	Wangaratta 1:250,000 Infill	872	1	1	0.5
200034	Buffalo Vic Infill UR2001/8	2	0.3	0.3	0.5
200035	Wangaratta Vic Infill UR2001/9	848	0.3	0.3	0.5
200132	Bogong and Omeo Area Vic Infill UR2001/12 29663	10	1	0.3	0.5
200133	Corryong Kosciuszko Rosewood Tallangatta Vic Infill	1175	1	0.3	0.5

3. Derivative products

As the data described in the previous section are not easily viewed and interpreted without geophysical knowledge and specialised software, various products that are depictions of the data have been created. These products comprise spatially referenced images, cross sections and vector shapefiles. Images are the main product type, and are made through assigning a colour scheme to the data as well as other image enhancement processes. Vector shapefiles allow point, line or polygon data to be displayed in a GIS such as the ESRI ArcGIS software package.

Images have been produced from the model-dependent earth conductivity predictions that were derived from the AEM survey data. These are described as plan and sectional views of conductivity. Image processed plan depictions of the gridded magnetic, gamma-ray, elevation and gravity data are also described. The location of the gravity survey stations is provided in an ESRI shapefile. All derivative products are stored in the projected coordinate system (Map Grid of Australia, Zone 55) using the Geocentric Datum of Australia 1994 (GDA94).

3.1 Glossary of image enhancement techniques

Many of the images described in the following sections have been enhanced using the same techniques. In order to understand the images produced, it is necessary to offer the following explanations for the common image enhancement techniques used. Further details on the enhancement and presentation of geophysical data are available in Milligan and Gunn (1997) and Milligan *et al.* (1992).

Colour look-up tables
Data can be displayed with different colour schemes, where values are assigned to (stretched between) 256 colours. The following colour schemes were used:

pseudocolour	varies from red (high) through yellow and cyan, to blue (low)
rainbow1	varies from white (high) through red, yellow, green, cyan and blue, to magenta (low)
rain_gomp	varies from magenta (high) through red, yellow, green and cyan, to blue (low)
greyscale	varies from white (high) through grey, to black (low)

Linear colour stretch
A linear colour stretch means that the range of input data values are mapped linearly to the 256 colours that are used in the look-up table. Linear colour stretched images that have the same data range can be easily compared (e.g. different conductivity depth slices).

Histogram equalised colour stretch
This is an enhancement where the range of data values is stretched and compressed so that all 256 colours in the look-up table occur with equal probability. Applying the histogram equalise transform changes an image so that no particular colour dominates, but that the whole range of colours are used to display the range of data values. This will highlight the

relative data variation across an image, though it makes absolute comparison of different images very difficult (e.g. each conductivity depth slice will have a unique colour stretch).

Logarithmic colour stretch
A logarithmic colour stretch means that the range of input data values are mapped logarithmically (base 10) to the 256 colours that are used in the look-up table. This assigns more colour variation to the lower data values than the higher data values.

Gradient enhancement
The gradient enhancement used on Billabong Creek data worked through applying a directional filter. All images with a gradient enhancement listed in Appendix E were produced with either an east-west (E-W) or northeast (NE) filter. Gradient enhancement accentuates the short wavelength information with artificial shadows, while still allowing the long wavelength information to be shown with a colour scheme. It introduces bias into an image, as structures that trend perpendicular to the illumination azimuth are enhanced more than others.

3.2 AEM products

To allow integration with subsurface information and facilitate better interpretation, the processed data from the AEM survey described in section 2.1 must be converted to conductivity as a function of horizontal location and position below the surface. The conversion can use either approximate transformation methods, or geophysical inverse modelling (inversion), both of which produce model-dependent conductivity predictions. It is generally the case that these conductivity predictions are non-unique: many different sets of conductivity predictions can be derived from the same data. One method of determining the reliability of conductivity predictions is to compare the predictions with an independent dataset, such as conductivity measurements from boreholes.

3.2.1 Previous AEM products

Model-dependent conductivity predictions were computed by Fugro from the HPRG corrected data. Detailed descriptions of the processing parameters were given in the acquisition and processing report for the AEM survey (Owers *et. al.*, 2002). The following two methods were used:

1. “Conductivity depth imaging” (CDI) via the software package EM Flow (version 4.00). The method is described by Macnae *et al.* (1998).
2. “Layered earth inversion” (LEI) via proprietary Fugro software. Sattel (1998) details this method.

In both of these methods, each observation point along a survey line was treated completely separately. They assumed the earth consists of a set of horizontal layers each having a constant electrical conductivity. For each observation point, the conductivities and thicknesses of the layers that would generate the observed response are determined. These results are non-unique and model- dependent. The following products were then derived from the model dependent conductivity predictions:

1. “Conductivity depth slices” or “Interval Conductivities” which represent the average of the predicted conductivity over a given depth range below surface.
2. “Conductive unit parameters” as described in Lane *et al.* (2000). This method identifies a conductive unit within the vertical conductivity profile and yields values for its

conductivity, thickness, and conductance, depth to its top and bottom and elevation (AHD) of its top and bottom.

In 2006 Geoscience Australia was contracted by BRS to determine whether the newly developed layered-earth inversion software (GA LEI) would provide better conductivity predictions than the Fugro products. Preliminary results indicated that the GA LEI software gave a substantially better product, and the complete dataset was inverted (Brodie and Fisher, 2008). The following section outlines the products generated by the GA LEI.

3.2.2 Geoscience Australia layered earth inversion (GA LEI)

The GA LEI process works by iteratively changing a starting model until the model has a calculated response that closely matches the observed data, with the end result being a point located dataset of conductivity at various depths. It differs from other methods in that, as well as solving for conductivity, it also solves for three parameters of the TEMPEST AEM system geometry that are not measured during the data acquisition. The technique can be described as a 1-dimensional smooth model inversion, where each sample point (measurement) is inverted independently (Figure 2). The method is summarised below from a more detailed description (Brodie and Fisher, 2008). The method has evolved from a similar approach that was used for the inversion of the Lower Balonne AEM survey (Lane *et al.*, 2004).

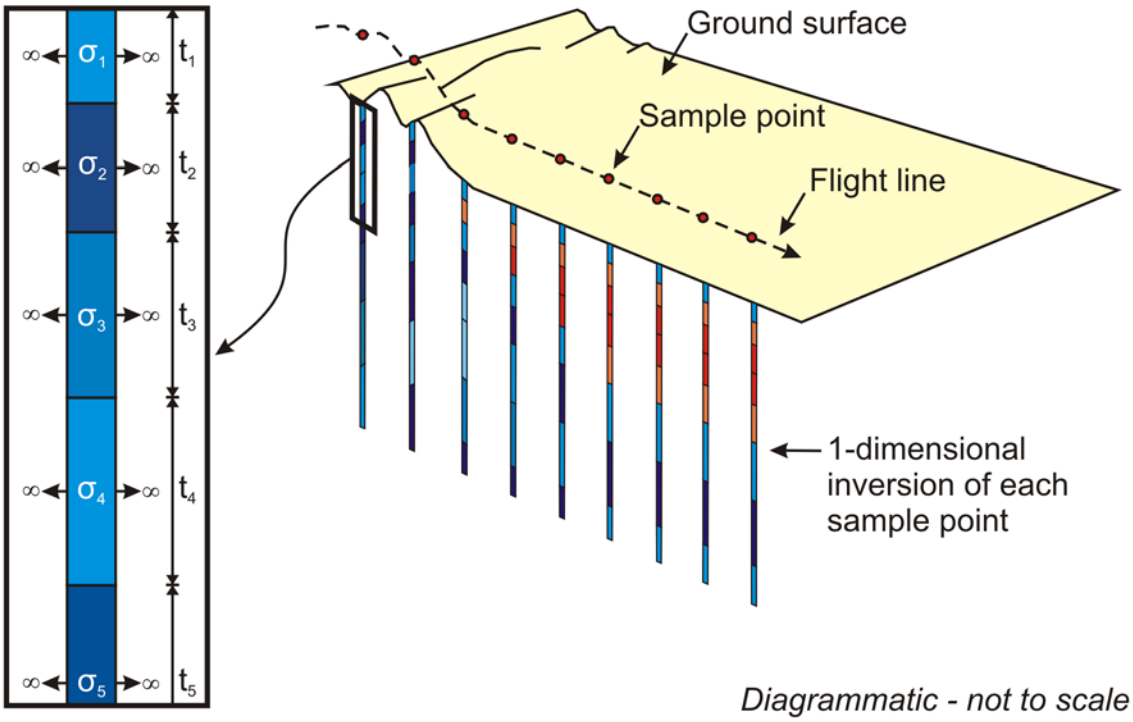

Figure 2 1-dimensional inversion with a vertically smooth model. Independent 1-dimensional models are calculated for each sample point along each flight line. The thickness of each layer (t_n) is fixed, and the conductivity (σ_n) is allowed to vary between layers, shown by the changing colours. Each 1-dimensional model assumes that the conductivity of each layer is laterally constant. Note that the diagram is not to scale and in reality sample points are ~12 m apart.

The conceptual model used in the AEM inversion was a 25 layer model with the first layer having a thickness of 2 m and each layer getting progressively thicker by 10% until the 24th layer had thickness 17.90 m and the 25th layer had infinite thickness. The layer thicknesses were kept fixed and the inversion solved for the conductivity of each layer. A reference model, whose conductivity varied both spatially and with depth, was used to constrain the layer conductivities. The reference model conductivity values were chosen via analysis of grids of total conductance generated from prior inversions of the data. Maximum smoothness (minimum roughness) constraints were imposed on the vertical conductivity profile at each inverted sample. The starting model in the inversion was identical to the reference model.

The inversion also solved for three parameters of the TEMPEST AEM system geometry that are not measured during the data acquisition. These were the in-line horizontal-and vertical separations between the transmitter and the receiver coils and the angular pitch of the receiver coils. Measured parameters of the system geometry, (transmitter height, pitch and roll), were taken to be the measured values and were not solved for. Other unmeasured geometry parameters (transmitter-receiver transverse separation, receiver roll and yaw), were assumed to be zero as there is insufficient information to solve for these parameters.

The following products were produced from the GA LEI and are present on the DVD compilation accompanying this report. For details on the image enhancements used, refer to Appendix E. The images can be viewed with any image viewing software, and as they are spatially referenced they can also be displayed using GIS software.

Conductivity distribution (point located [or line] data)
The results of the GA LEI are stored in a point located (or line) format, in an ASCII (.dat) file formatted with space-delimited columns. Each record represents one sample along a flight line, which records the conductivity values for the modelled layers. A comprehensive header file (.hdr) is associated with the file, which describes the data and the numeric format of each column in the file.

Conductivity depth sections
Enhanced images of vertical conductivity depth sections along each flight line were produced from the GA LEI results. These were produced by first applying a five point (~62m) along line median filter to the independent 1-dimensional inversion results, before stitching them into the vertical sections of conductivity (Figure 3). The sections were outputted as coloured images in JPEG and PDF formats, with a horizontal scale of 1:100 000 and a vertical scale of 1:5 000 (vertical exaggeration of 20). These scales are only relevant when viewing the products at their original page/image size. A colour scale is included, as is the location (eastings and northings) of each flight line. Two sets of sections were produced: one using a pseudocolour linear colour stretch using a data range of 0-0.5 S/m and the other using a pseudocolour logarithmic colour stretch using a data range of 0.01-1 S/m.

Conductivity layers and depth slices (grids and images)
The results of the GA LEI were converted into grids of conductivity (S/m) for each of the 25 layers in the GA LEI model. The results were also converted into grids of conductivity for depthslices, over the following range of depths: 0-5m, 5-10m, 10-15m, 15-20m, 20-30m, 30-40m, 40-60m, 60-80m, 80-100m, 100-150m, and 150-200m. The conductivity values in each depth-slice were calculated as a weighted average of the corresponding layers outputted from the GA LEI (Figure 4). They were produced as binary *ERMapper* single band IEEE4Byte

Real data files with a comprehensive header (.ers) file that describes the data and the geographic positioning of the grid.

Enhanced images of the grids were also produced as JPEG image files (.jpg) with associated world files (.jgw) that hold the spatial reference information. These images also include an embedded scale bar that show how the colours correspond to conductivity values (Figure 5). Two sets of images were produced: one using a pseudocolour histogram equalised colour stretch with an E-W gradient; the other using a pseudocolour linear colour stretch with an E-W gradient. The images created using the histogram equalised colour stretch stop at 100m depth because the lower two depth slice grids (100-150m and 150-200m) have very small data value ranges, and the histogram equalise colour stretch would create a misleading depiction of the data (e.g. the image would be dominated by noise rather than signal).

Conductance distribution (grids and images)
A grid and images of conductance were produced from the GA LEI results. Conductance is conductivity multiplied by thickness, and is measured in siemens (S). The grid was produced as a binary *ERMapper* single band IEEE4Byte Real data file with a comprehensive header (.ers) file that describes the data and the geographic positioning of the grid. Two images were produced: one using a pseudocolour linear colour stretch with an E-W gradient; the other using pseudocolour histogram equalised colour stretch with an E-W gradient. Both images include an embedded scale bar that show how the colours correspond to conductance values that range from 0 to 30 S.

Base of the conductive unit (grids and images)
An automated technique was applied to the point located GA LEI to create products based on the depth of the base of the conductive unit. This technique worked from the bottom up, and picked the first point at which a conductivity threshold value is exceeded. For Billabong Creek a threshold value of 0.100 S/m was used. If it is assumed that the conductive material above the threshold value represents transported and *in situ* regolith, then the base of the conductive unit corresponds to the depth of basement. This assumption has not been tested and may not be valid.

Applying this technique resulted in the production of two grids: elevation of the base of the conductive unit; and, depth of the base of the conductive unit below the ground surface. The grids were produced as binary *ERMapper* single band IEEE4Byte Real data file with comprehensive header (.ers) files that describe the data and the geographic positioning of the grid. The grids were subjected to filtering and micro-levelling to reduce noise.

The grids were then subject to image enhancement, producing JPEG files with associated world files (.jgw) that hold the spatial reference information. These images include an embedded scale bar that show how the colours correspond to elevation or depth values. Two images were produced: one using a rainbow1 linear colour stretch with an E-W gradient of the depth of the conductive layer; the other using a rainbow1 linear colour stretch with an E-W gradient of elevation of the conductive layer.

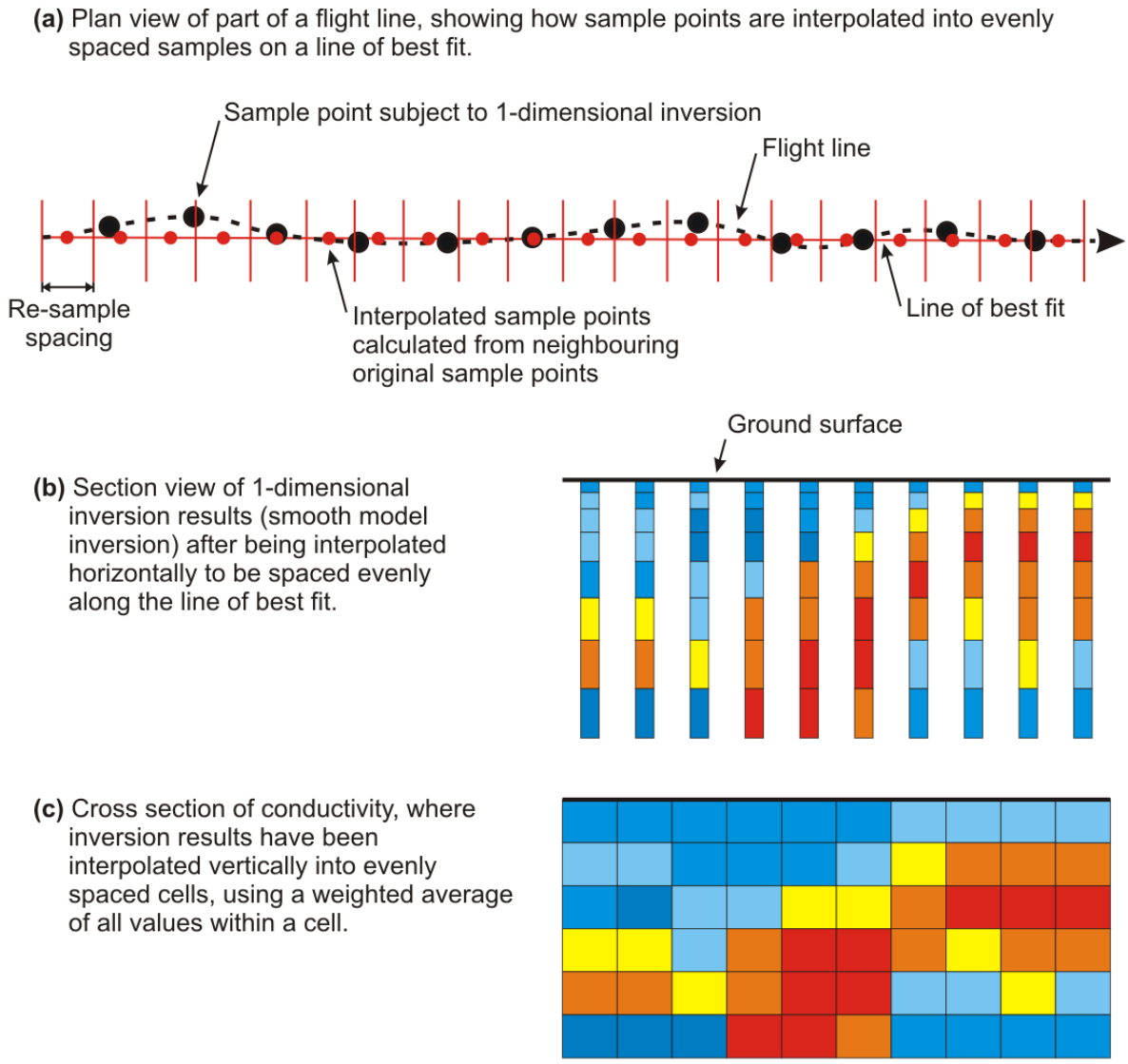

Figure 3 Creating flight-line conductivity-depth sections from the modelled conductivity predictions. The sample points are first interpolated horizontally onto a line of best fit (a). The inversion results (b) are then interpolated vertically (c) into an evenly spaced grid. Note that the sample points are spaced every ~12 m along the line. A horizontal five point median filter is applied to each layer.

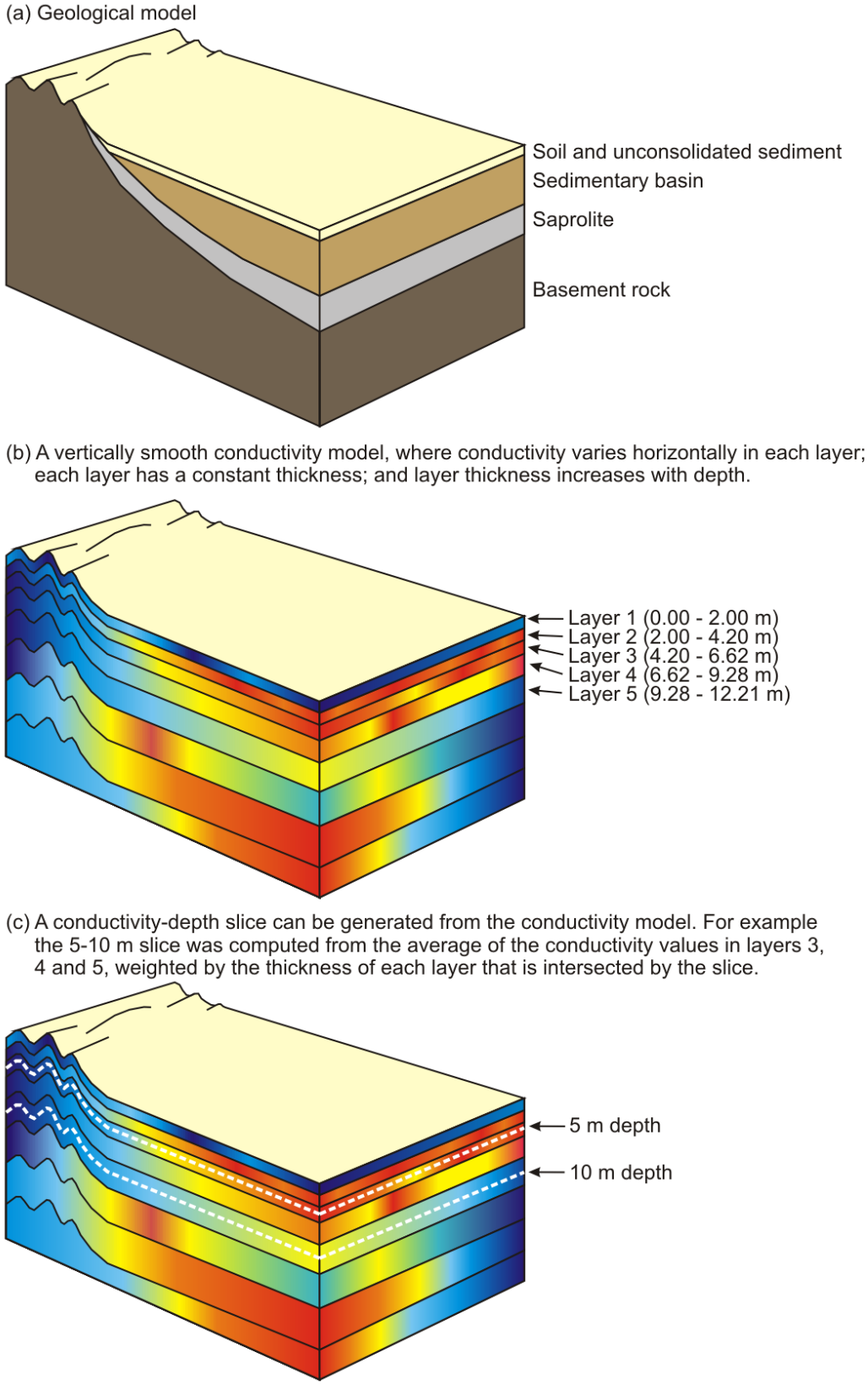

Figure 4 Creating conductivity-depth slices from the modelled conductivity predictions.

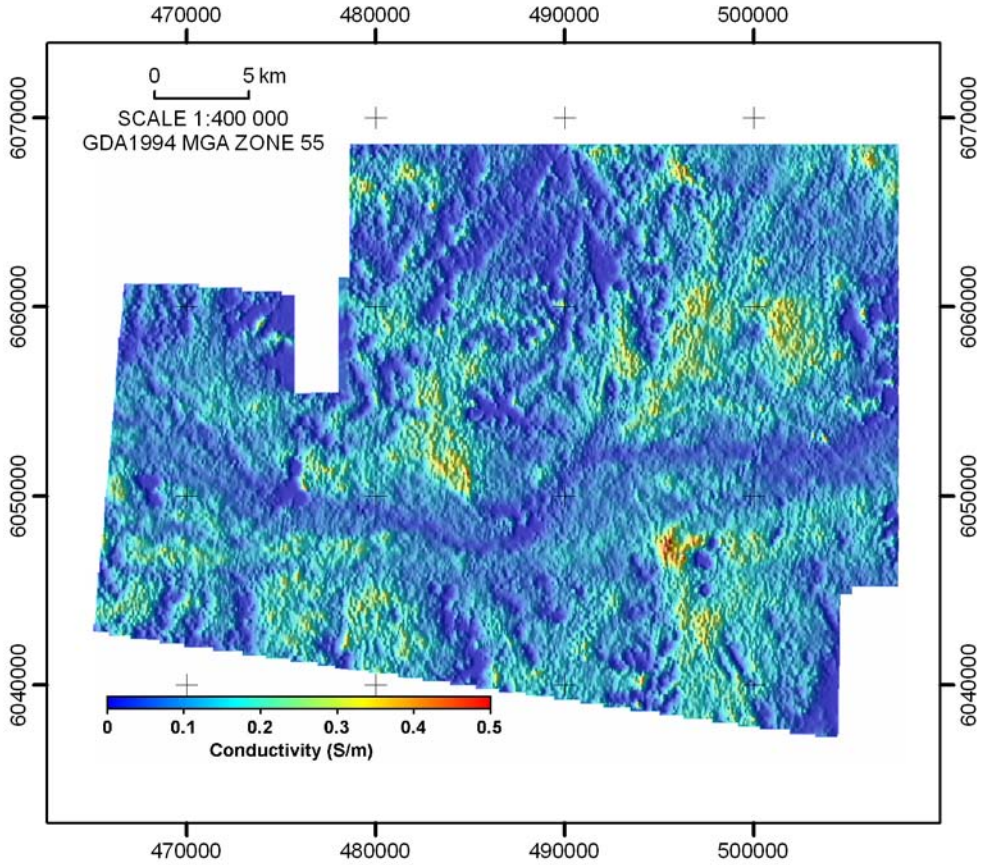

Figure 5 Conductivity-depth slice (pseudocolour linear colour stretch with an E-W gradient enhancement) for 0-5 m depth from the GA LEI of the Billabong Creek AEM data.

3.3 Magnetic products

Section 2.2 describes the different grids that were produced of different aspects of the Billabong Creek magnetic data, including such aspects as the data extent and lineage. This section describes the methods used to create images that were derived from these grids, which can be used as enhanced depictions of the data.

The images were produced in the *ERMapper* software package, and exported in the JPEG (.jpg) format, including associated world files (.jgw) that contain spatial reference information. The images can be viewed with any image viewing software, and as they are spatially referenced they can also be displayed using GIS. Each image is briefly described below, while the details of all the derivative products are in Appendix E.

Total magnetic intensity (TMI)
Two images of the TMI gridded data were produced: one is a simple histogram equalised image using the raingomp colour look-up-table; the other uses an enhancement technique described in Milligan and Gunn (1997) that combines a gradient enhancement (NE filter) and a colour image (pseudocolour histogram equalised) in the hue-saturation-intensity colour space. The TMI images show variations in the amplitude of the magnetic field, due to the spatial distribution and concentration of magnetically significant minerals. The images include an embedded scale bar that show how the colours correspond to values of residual total magnetic intensity (nT).

Total magnetic intensity – reduced to the pole (TMI-RTP)
Two images of the TMI-RTP gridded data were produced: one is a simple histogram equalised image using the raingomp colour look-up-table; the other uses an enhancement technique described in Milligan and Gunn (1997) that combines a gradient enhancement (NE filter) and a colour image (pseudocolour histogram equalised) in the hue-saturation-intensity colour space (Figure 6). These are images of TMI data that have been reduced to the pole (RTP). This is a post-processing technique performed on the gridded data (see section 2.2) that removes the asymmetry in TMI data that is caused by the non-vertical inclination of the Earth's magnetic field. This simplifies the images so that induced magnetic anomalies from vertical sources are located over the geological body responsible, rather than being skewed and offset to one side. The images include an embedded scale bar that show how the colours correspond to values of residual total magnetic intensity reduced to the pole (nT).

Total magnetic intensity – reduced to the pole – first vertical derivative (TMI-RTP-VD1)
Two images of the TMI-RTP-VD1 gridded data were produced: one is a simple pseudocolour histogram equalised image, while the other is a simple greyscale histogram equalised image. These are images of the first vertical derivative of the TMI-RTP data. This is a post-processing technique performed on the gridded data (see section 2.2) that quantifies the spatial rate of change of the magnetic field in the vertical direction. It essentially enhances the high frequency anomalies relative to low frequencies.

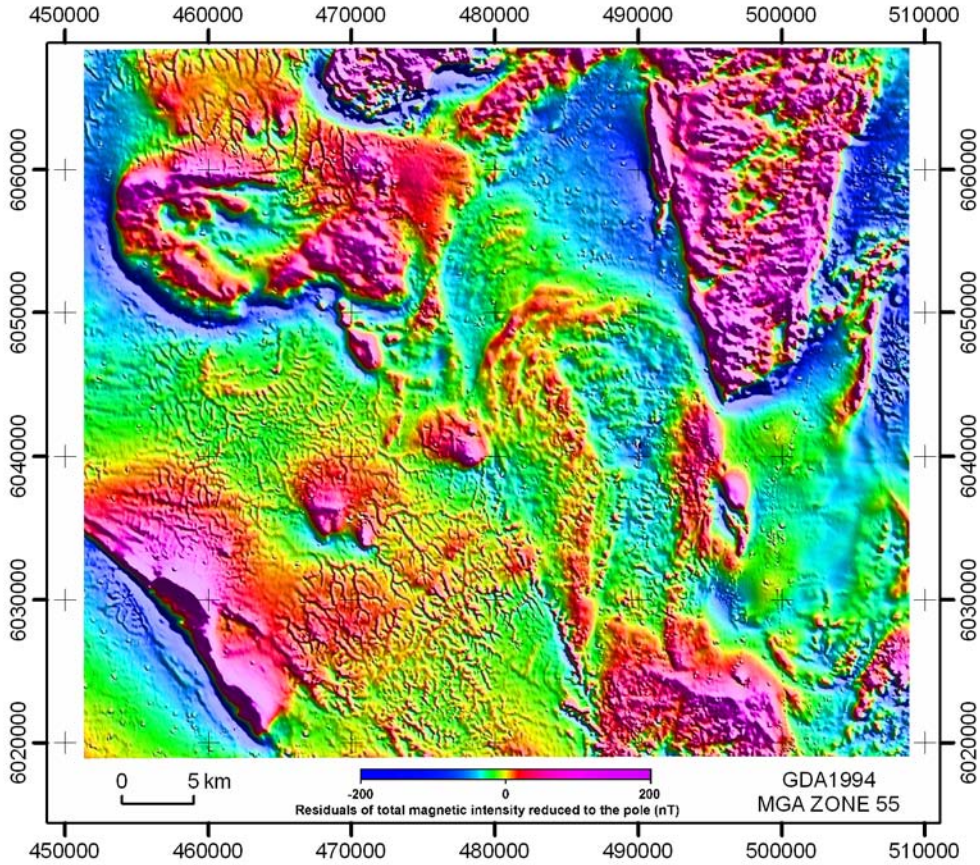

Figure 6 Enhanced image of TMI-RTP from the Billabong Creek MAGSPEC survey data.

3.4 Gamma-ray products

Section 2.2 describes the different grids that were produced of different aspects of the Billabong Creek gamma-ray data, including such aspects as the data extent and lineage. This section describes the methods used to create images that were derived from these grids, and which can be used as enhanced depictions of the data.

The images were produced in the *ER Mapper* software package, and exported in the JPEG (.jpg) format, including associated world files (.jgw) that contain spatial reference information. The images can be viewed with any image viewing software, and as they are spatially referenced they can also be displayed using GIS. Each image is briefly described below, while the details of all the derivative products are in Appendix E.

K-Th-U ternary
A ternary image was produced showing potassium in red, thorium in green and uranium in blue (Figure 7). The datasets were each histogram equalised as they were combined in the red-green-blue colour space. The image includes an embedded diagram that shows how the colours correspond to the different datasets.

Dose rate
An enhanced colour image of the dose rate gridded data was produced combining a raingomp colour look up table with a histogram equalised colour stretch and an NE gradient filter. The image includes an embedded scale bar that shows how the colours correspond to the values of dose rate (nG/hr).

Potassium
An enhanced colour image of the potassium gridded data was produced combining a raingomp colour look up table with a histogram equalised colour stretch and an NE gradient filter. The image includes an embedded scale bar that shows how the colours correspond to the values of equivalent potassium concentration (%).

Thorium
An enhanced colour image of the thorium gridded data was produced combining a raingomp colour look up table with a histogram equalised colour stretch and an NE gradient filter. The image includes an embedded scale bar that shows how the colours correspond to the values of equivalent thorium concentration (eppm).

Uranium
An enhanced colour image of the uranium gridded data was produced combining a raingomp colour look up table with a histogram equalised colour stretch and an NE gradient filter. The image includes an embedded scale bar that shows how the colours correspond to the values of equivalent uranium concentration (eppm).

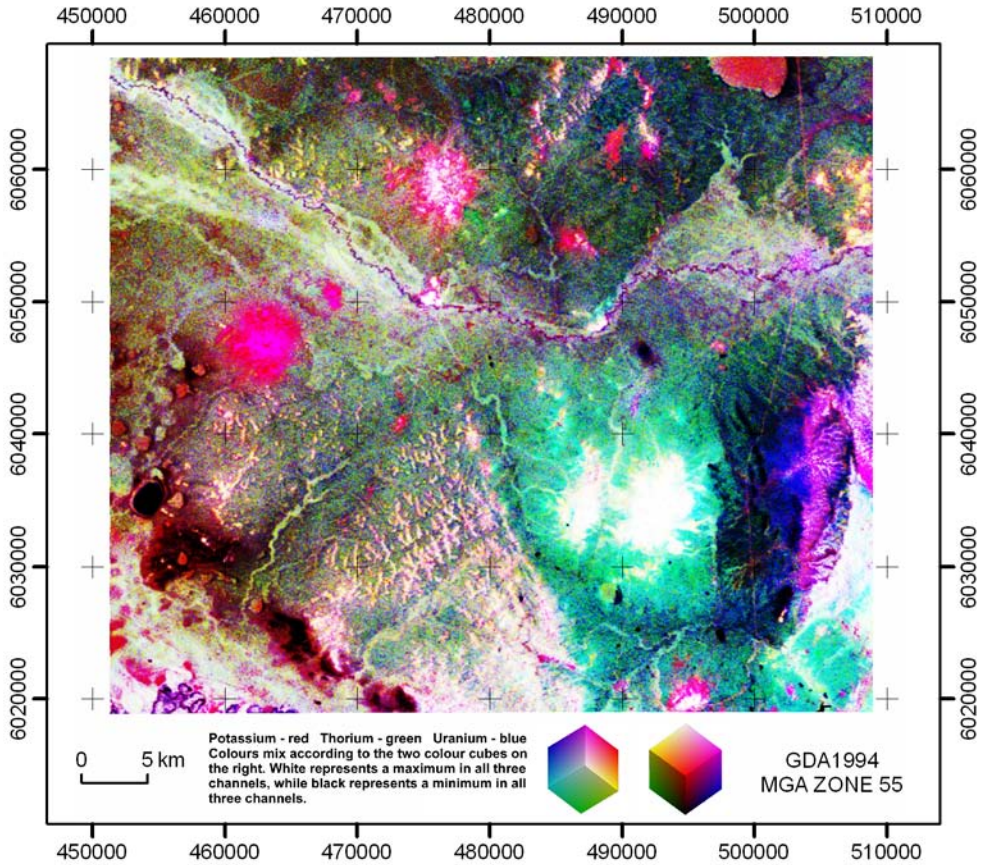

Figure 7 Enhanced ternary gamma-ray image from the Billabong Creek MAGSPEC survey data.

3.5 DEM products

Section 2.2 describes the different grids that were produced of different aspects of the Billabong Creek elevation data, including such aspects as the data extent and lineage. This section describes the methods used to create products that were derived from these grids, and which can be used as enhanced depictions of the data. Details of the derivative products are in Appendix E.

DEM enhanced image

A colour enhanced image of the gridded elevation data was produced using the rainbow1 colour look up table, histogram equalised colour stretch and a NE gradient (Figure 8).It was created in the *ER Mapper* software package, and exported in the JPEG (.jpg) format, including associated world files (.jgw) that contain spatial reference information. The image can be viewed with any image viewing software, and as it is spatially referenced it can also be displayed using GIS software. The image includes an embedded scale bar that shows how the colours correspond to the values of elevation (m).

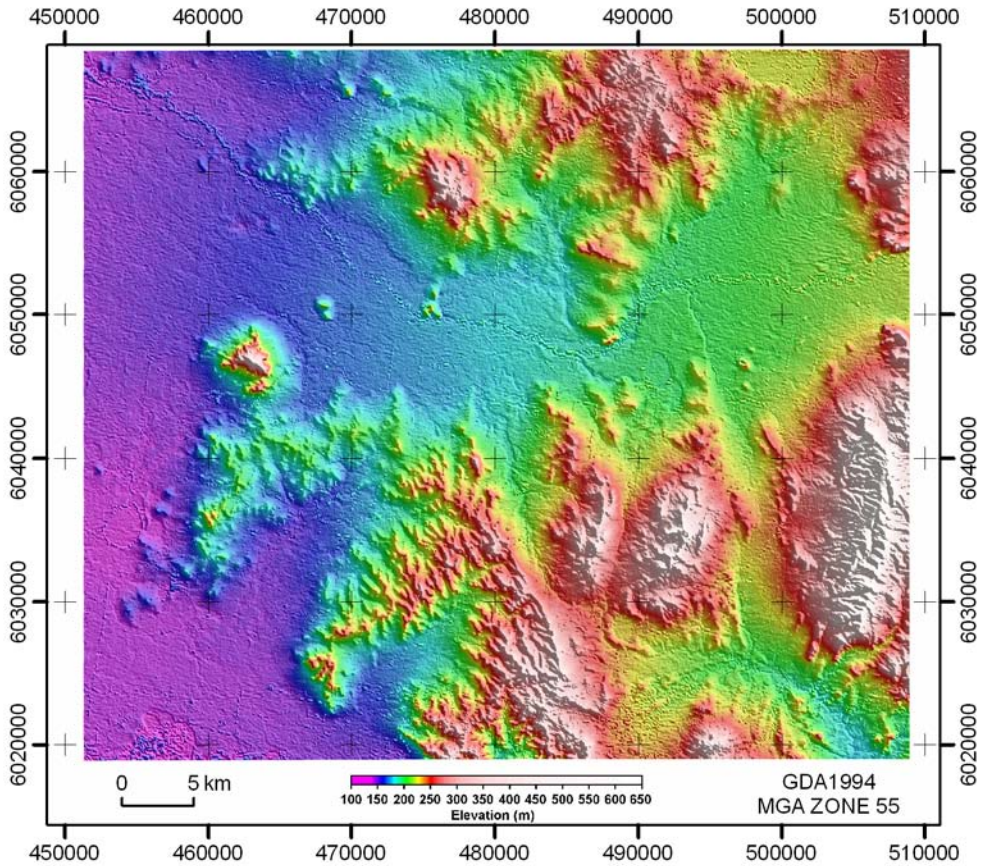

Figure 8 Enhanced DEM image from the Billabong Creek MAGSPEC survey data.

3.6 Gravity products

Section 2.3 describes the grid that was produced from the Billabong Creek gravity data, including such aspects as the data extent and lineage. This section describes the methods used to create products that were derived from these grids, and which can be used as enhanced depictions of the data. Details of the derivative products are in Appendix E.

3.6.1 Enhanced gravity image

Using the *ER Mapper* software package, a colour enhanced image of the regional gridded gravity data was produced and exported in the JPEG (.jpg) file format with associated world file (.jgw). The image was produced using a pseudocolour histogram equalised colour stretch with a northeast gradient. As the enhanced image looked particularly poor using the grids cell size of 2 km, the grid was subsampled to 500 m using the *Intrepid* software package (version 4.1) before enhancing. A second enhanced image was also produced of a smaller subset of the regional grid. This image only covers the MAGSPEC survey boundary and provides a slightly clearer view of the relative changes in observed gravity across the area of interest; however it is still a coarse image due to the wide spacing of survey stations (Figure 9).

3.6.2 Gravity station shapefile

Using the *Intrepid* software package (version 4.1) an ArcGIS shapefile of the location of the gravity survey stations used to create the gridded gravity data was produced (Figure 9). This shows the irregular spacing of around 10 km between gravity stations, which results in the coarse resolution of the grid.

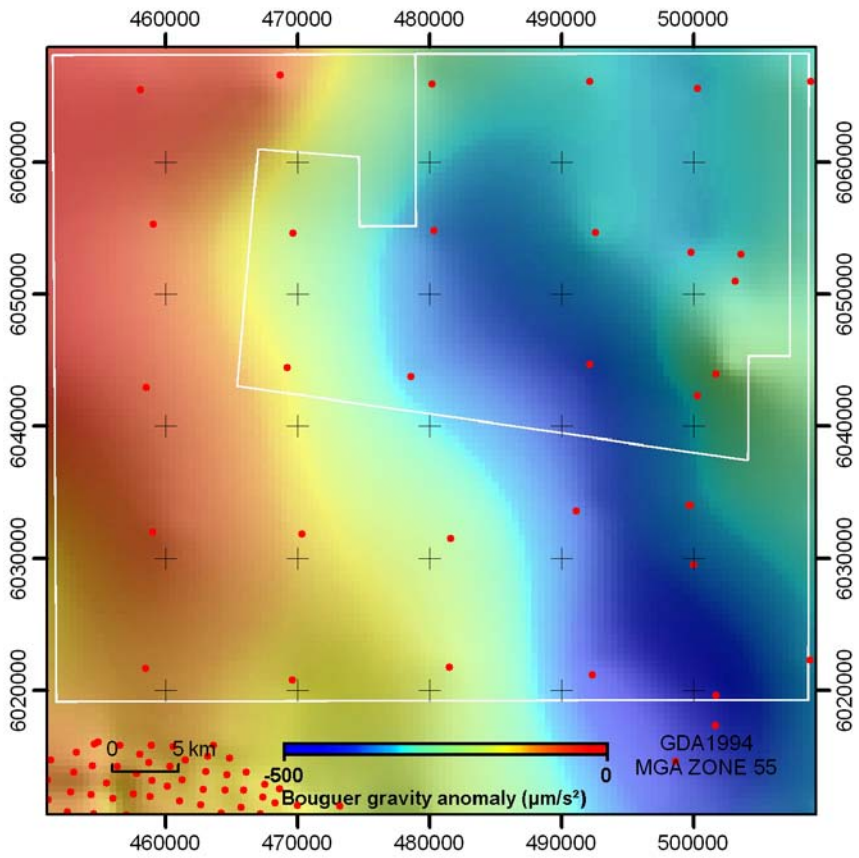

Figure 9 Enhanced image of Bouguer gravity anomaly data and the location of gravity survey stations (red dots) for the Billabong Creek area.

References

Brodie, R and Fisher, A (2008) Inversion of TEMPEST AEM survey data, Billabong Creek, New South Wales. Unpublished report produced by Geoscience Australia for the Bureau of Rural Sciences.

Grasty, R.L. and Minty, B.R.S, 1995. A Guide To The Technical Specifications For a Airborne Gamma-Ray Survey. AGSO Record 1995/60.

Green, A (1998) Altitude correction of time domain AEM data for image display and geological mapping, using the Apparent Dipole Depth (ADD) method. *Exploration Geophysic*s, 29, 87-91

Heiskanen, W.A., and Moritz, H., 1967. Physical Geodesy. W.H. Freeman and Company.

Horsfall, KR (1997) Airborne magnetic and gamma-ray data acquisition. *AGSO Journal of Geology and Geophysics*, 17, 23-30.

Hovgaard, J and Grasty, RL (1997) Reducing noise in airborne gamma-ray data through spectral component analysis. Exploration 97, Ontario Geological Survey.

Kevron Geophysics (2001) Operations and processing report, Honeysuckle Creek and Billabong Creek geophysical surveys. Unpublished Kevron Geophysics report to the Bureau of Rural Sciences.

LaFehr, T.R., 1991. An exact solution for the gravity curvature (Bullard B) correction. *Geophysics*, 56, 1179-1184.

Lane, R, Brodie, R and Fitzpatrick, A (2004) Constrained inversion of AEM data from the Lower Balonne area, Southern Queensland, Australia: CRC LEME Open File Report 163.

Lane, R, Green, A, Golding, C, Owers, M, Pik, P, Plunkett, C, Sattel, D and Thorn, B (2000) An example of 3-D conductivity mapping using the TEMPEST airborne electromagnetic system. *Exploration Geophysics*, 31, 162-172

Macnae, JC, King, A, Stolz, N, Osmakoff, A and Blaha, A (1998) Fast AEM data processing and inversion. *Exploration Geophysics*, 29, 163-169.

Milligan, PR and Gunn, PJ (1997) Enhancement and presentation of airborne geophysical data. *AGSO Journal of Geology and Geophysics*, 17, 63-75.

Milligan, PR, Morse, MP and Rajagopalan, S (1992) Pixel map preparation using the HSV colour model. Exploration Geophysics, 23, 219-224.

Mohr, P. J., and Taylor, B.N., 2001. The Fundamental Physical Constants. *Physics Today*, 54, 6-16.

Moritz, H., 1980. Geodetic Reference System 1980. *Journal of Geodesy*, 54, 395-405.

Owers, M, Sattel, D and Stenning, L (2002) Billabong Creek, New South Wales, acquisition and processing report. Unpublished Fugro Airborne Surveys report to the Bureau of Rural Sciences.

Sattel, D (1998) Conductivity information in three dimensions. *Exploration Geophysics*, 29, 157-162.

Wenzel, H., 1985. Hochauflosende Kugelfunktionsmodelle fur des Gravitationspotential der Erde [1]: Wissenschaftliche arbeiten der Fachrichtung Vermessungswesen der Universitat Hannover, 137.

Appendix A – Technical specifications of the AEM survey and system

Table A.1 Technical specifications of the Billabong Creek AEM survey from Owers *et al.* (2002).

Aircraft:	CASA C212-200 Turbo Prop, VH-TEM
Flight line spacing:	200 metres
Tie line spacing:	Tielines not flown
Flight line direction:	east-west
Tie line direction:	Tielines not flown
Survey distance:	5 522 kilometres
Terrain clearance:	120 metres (nominal)
Along line sampling:	0.2 seconds (~12 metres) magnetics 1.0 seconds (~60 metres) GPS 13.333 microseconds streamed AEM 0.2 seconds (~12 metres) stacked AEM

Table A.2 Technical specifications of the AEM (TEMPEST) system from Lane *et al.* (2000).

Base frequency:	25Hz
Transmitter area:	244m2
Transmitter turns:	1
Waveform:	Square
Duty cycle:	50%
Transmitter pulse width:	10 ms
Transmitter off-time:	10 ms
Peak current:	300 A
Peak moment:	73,200 Am2
Average moment:	36,600 Am2
Sample rate:	75 kHz
Sample interval:	13.33 microseconds
Samples per half-cycle:	1500
System bandwidth:	25 Hz to 37.5 kHz
EM receiver:	Towed bird with 3 component dB/dt coils (X and Z components are recorded and processed)
Tx-Rx horizontal separation:	120m (nominal)
Tx-Rx vertical separation:	30m (nominal)
Stacked data output interval:	200 ms (~12 m)
Number of output windows:	15
Window centre times:	13 µs to 16.2 ms
Magnetometer:	Stinger-mounted caesium vapour
Magnetometer compensation:	fully digital
Magnetometer output interval:	200 ms (~12 m)
Magnetometer resolution:	0.001nT
Typical noise level:	0.2nT
GPS cycle rate:	1 second

Appendix B – Technical specifications of the MAGSPEC survey and system

Table B.1 Technical specifications of the MAGSPEC survey from Kevron Geophysics (2001).

Aircraft:	Aerocommander Shrike, VH-KAV
Flight line spacing:	100 metres
Tie line spacing:	1000 metres
Flight line direction:	east-west
Tie line direction:	north-south
Survey distance:	34 178 kilometres
Nominal flying height:	60 metres above ground level
Along line sampling:	0.1 seconds (~7 metres) magnetics
	1.0 seconds (~70 metres) gamma-ray
	1.0 seconds (~70 metres) GPS
	0.1seconds (~7 metres) altimeter

Table B.2 Technical specifications of the MAGSPEC system Kevron Geophysics (2001).

Aircraft Magnetometer:	Geometrics G-822A Caesium vapour
Magnetic Compensator:	RMS Instruments Automatic Aeromagnetic Digital Compensator (AADC)
Base station magnetometer:	Geometrics G856 proton precession
Gamma-ray spectrometer:	Exploranium GR820, 256 channels
Gamma-ray detector:	NaI(T1) crystals; 50 L down
Altimeter:	Sperry AA-210 radio altimeter
Barometer:	Rosemount 1241m
Thermometer:	Rosemount Model 2200 temperature sensor
Navigation system:	Fugro Omnistar Virtual Base Station mode with 12 Ashtech GPS receiver.
Flight Track Recording:	VHS video tracking camera with wide-angle lens
Data acquisition system:	RMS Instruments DAS-8 digital acquisition system

Appendix C – Airborne geophysical survey boundary coordinates

Table C.1 Vertices of the boundary polygon of the Billabong Creek AEM survey.

Longitude (^{o}E)	Latitude (^{o}S)
147.081	35.529
146.768	35.529
146.768	35.647
146.721	35.647
146.721	35.600
146.636	35.594
146.618	35.756
147.046	35.807
147.047	35.736
147.081	35.736

Appendix D – Technical specifications of map projections

Projection Name:	Map Grid of Australia, Zone 55
Units:	Metres
Datum:	Geocentric Datum of Australia 1994 (GDA94)
Epoch:	1994.0
Ellipsoid:	GRS80
Semi-major axis (a):	6 378 137.0 metres
Inverse flattening (1/f):	298.257222101
Central meridian	147°00’00’’
False Easting:	500 000 metres
False Northing:	10 000 000 metres

Appendix E – Data stored on the accompanying DVD

Folder 1 (survey)	Folder 2 (format)	Folder 3\4 (data type)	File name	File description
AEM	line_data		billabong_creek_tempest.dat	final point located data from the AEM survey (see .hdr file for details)
			billabong_creek_inversion.dat	final point located AEM data produced by the GA-LEI (see .hdr file for details)
	grids	conductance	conductance_000m_200m.ers	40 m grid of conductance between 0-200 m depth derived from the GA LEI
		conductivity_base	conductivity_base_depth.ers	40 m grid of the depth of the base of the conductive layer derived from the GA LEI
			conductivity_base_elevation.ers	40 m grid of elevation of the base of the conductive layer derived from the GA LEI
		depthslices	depthslice_000m_005m.ers	40 m grid of conductivity in the 0-5 m depth slice produced by the GA-LEI
			depthslice_005m_010m.ers	40 m grid of conductivity in the 5-10 m depth slice produced by the GA-LEI
			depthslice_010m_015m.ers	40 m grid of conductivity in the 10-15 m depth slice produced by the GA-LEI
			depthslice_015m_020m.ers	40 m grid of conductivity in the 15-20 m depth slice produced by the GA-LEI
			depthslice_020m_030m.ers	40 m grid of conductivity in the 20-30 m depth slice produced by the GA-LEI
			depthslice_030m_040m.ers	40 m grid of conductivity in the 30-40 m depth slice produced by the GA-LEI
			depthslice_040m_060m.ers	40 m grid of conductivity in the 40-60 m depth slice produced by the GA-LEI
			depthslice_060m_080m.ers	40 m grid of conductivity in the 60-80 m depth slice produced by the GA-LEI
			depthslice_080m_100m.ers	40 m grid of conductivity in the 80-100 m depth slice produced by the GA-LEI
			depthslice_100m_150m.ers	40 m grid of conductivity in the 100-150 m depth slice produced by the GA-LEI
			depthslice_150m_200m.ers	40 m grid of conductivity in the 150-200 m depth slice produced by the GA-LEI
		layers	layer_01.ers	40 m grid of conductivity for layer 1 (0.00-2.00 m) produced by the GA-LEI
			layer_02.ers	40 m grid of conductivity for layer 2 (2.00-4.20 m) produced by the GA-LEI
			layer_03.ers	40 m grid of conductivity for layer 3 (4.20-6.62 m) produced by the GA-LEI
			layer_04.ers	40 m grid of conductivity for layer 4 (6.62-9.28 m) produced by the GA-LEI
			layer_05.ers	40 m grid of conductivity for layer 5 (9.28-12.21 m) produced by the GA-LEI
			layer_06.ers	40 m grid of conductivity for layer 6 (12.21-15.43 m) produced by the GA-LEI
			layer_07.ers	40 m grid of conductivity for layer 7 (15.43-18.97 m) produced by the GA-LEI
			layer_08.ers	40 m grid of conductivity for layer 8 (18.97-22.87 m) produced by the GA-LEI
			layer_09.ers	40 m grid of conductivity for layer 9 (22.87-27.16 m) produced by the GA-LEI
			layer_10.ers	40 m grid of conductivity for layer 10 (27.16-31.87 m) produced by the GA-LEI
			layer_11.ers	40 m grid of conductivity for layer 11 (31.87-37.06 m) produced by the GA-LEI
			layer_12.ers	40 m grid of conductivity for layer 12 (37.06-42.77 m) produced by the GA-LEI
			layer_13.ers	40 m grid of conductivity for layer 13 (42.77-49.04 m) produced by the GA-LEI
			layer_14.ers	40 m grid of conductivity for layer 14 (49.04-55.95 m) produced by the GA-LEI
			layer_15.ers	40 m grid of conductivity for layer 15 (55.95-63.54 m) produced by the GA-LEI
			layer_16.ers	40 m grid of conductivity for layer 16 (63.54-71.90 m) produced by the GA-LEI
			layer_17.ers	40 m grid of conductivity for layer 17 (71.90-81.09 m) produced by the GA-LEI
			layer_18.ers	40 m grid of conductivity for layer 18 (81.09-91.20 m) produced by the GA-LEI

Folder 1 (survey)	Folder 2 (format)	Folder 3\4 (data type)	File name	File description
AEM	grids	layers	layer_19.ers	40 m grid of conductivity for layer 19 (91.20-102.32 m) produced by the GA-LEI
			layer_20.ers	40 m grid of conductivity for layer 20 (102.32-114.55 m) produced by the GA-LEI
			layer_21.ers	40 m grid of conductivity for layer 21 (114.55-128.00 m) produced by the GA-LEI
			layer_22.ers	40 m grid of conductivity for layer 22 (128.00-142.80 m) produced by the GA-LEI
			layer_23.ers	40 m grid of conductivity for layer 23 (142.80-159.09 m) produced by the GA-LEI
			layer_24.ers	40 m grid of conductivity for layer 24 (159.09-176.99 m) produced by the GA-LEI
			layer_25.ers	40 m grid of conductivity for layer 25 (176.99-∞ m) produced by the GA-LEI
	images	conductivity_base	conductivity_base_depth_linear.jpg	rainbow1 linear stretch with a E-W gradient of interpreted basement depth
			conductivity_base_elevation_linear.jpg	rainbow1 linear stretch with a E-W gradient of interpreted basement elevation
		conductance	conductance_000m_200m_linear.jpg	pseudocolour linear stretch with a E-W gradient of the conductance grid
			conductance_000m_200m_he.jpg	pseudocolour histogram equalised with a E-W gradient of the conductance grid
		depthslices\he	depthslice_000m_005m_he.jpg	pseudocolour histogram equalised with a E-W gradient of the conductivity depth slice
			depthslice_005m_010m_he.jpg	pseudocolour histogram equalised with a E-W gradient of the conductivity depth slice
			depthslice_010m_015m_he.jpg	pseudocolour histogram equalised with a E-W gradient of the conductivity depth slice
			depthslice_015m_020m_he.jpg	pseudocolour histogram equalised with a E-W gradient of the conductivity depth slice
			depthslice_020m_030m_he.jpg	pseudocolour histogram equalised with a E-W gradient of the conductivity depth slice
			depthslice_030m_040m_he.jpg	pseudocolour histogram equalised with a E-W gradient of the conductivity depth slice
			depthslice_040m_060m_he.jpg	pseudocolour histogram equalised with a E-W gradient of the conductivity depth slice
			depthslice_060m_080m_he.jpg	pseudocolour histogram equalised with a E-W gradient of the conductivity depth slice
			depthslice_080m_100m_he.jpg	pseudocolour histogram equalised with a E-W gradient of the conductivity depth slice
		depthslices\lin	depthslice_000m_005m_linear.jpg	pseudocolour linear stretch with a E-W gradient of the conductivity depth slice
			depthslice_005m_010m_linear.jpg	pseudocolour linear stretch with a E-W gradient of the conductivity depth slice
			depthslice_010m_015m_linear.jpg	pseudocolour linear stretch with a E-W gradient of the conductivity depth slice
			depthslice_015m_020m_linear.jpg	pseudocolour linear stretch with a E-W gradient of the conductivity depth slice
			depthslice_020m_030m_linear.jpg	pseudocolour linear stretch with a E-W gradient of the conductivity depth slice
			depthslice_030m_040m_linear.jpg	pseudocolour linear stretch with a E-W gradient of the conductivity depth slice
			depthslice_040m_060m_linear.jpg	pseudocolour linear stretch with a E-W gradient of the conductivity depth slice
			depthslice_060m_080m_linear.jpg	pseudocolour linear stretch with a E-W gradient of the conductivity depth slice
			depthslice_080m_100m_linear.jpg	pseudocolour linear stretch with a E-W gradient of the conductivity depth slice
			depthslice_100m_150m_linear.jpg	pseudocolour linear stretch with a E-W gradient of the conductivity depth slice
			depthslice_150m_200m_linear.jpg	pseudocolour linear stretch with a E-W gradient of the conductivity depth slice

Folder 1 (survey)	Folder 2 (format)	Folder 3\4 (data type)	File name	File description
AEM	sections	log_0.01_1.00\jpg	20010.log_0.01_1.00.jpg	pseudocolour logarithmic stretch conductivity-depth section of the 181 flightlines
		log_0.01_1.00\pdf	20010.log_0.01_1.00.pdf	as above, in pdf format
		linear_0.0_0.5\jpg	20010.linear_0.0_0.5.jpg	pseudocolour linear stretch conductivity-depth section of the 181 flightlines
		linear_0.0_0.5\pdf	20010.linear_0.0_0.5.pdf	as above, in pdf format
MAGSPEC	grids	dem	billabong_dem_magspec.ers	20m grid of elevation, derived from MAGSPEC survey
		mag	billabong_tmi.ers	20 m grid of total magnetic intensity (TMI)
			billabong_tmirtp.ers	20 m grid of TMI reduced to the pole (RTP)
			billabong_tmirtpvd1.ers	20 m grid of the 1st vertical derivative (VD1) of the TMI RTP
		rad	billabong_dose.ers	20 m grid of dose rate data (nG.hr^{-1}), derived from total count channel
			billabong_potassium.ers	20 m grid of equivalent concentration of potassium (percent)
			billabong_thorium.ers	20 m grid of equivalent concentration of thorium (eppm)
			billabong_uranium.ers	20 m grid of equivalent concentration of uranium (eppm)
	images	dem	dem_magspec_enhanced.jpg	rainbow1 histogram equalised image of elevation with a NE gradient
		mag	tmi_raingomp.jpg	rain-gomp histogram equalised image of TMI
			tmi_hsi_enhanced.jpg	rain_gomp histogram equalised image of TMI with a NE gradient
			tmirtp_raingomp.jpg	rain-gomp histogram equalised image of TMI RTP
			tmirtp_hsi_enhanced.jpg	rain_gomp histogram equalised image of TMI RTP with a NE gradient
			tmirtpvd1_grey.jpg	greyscale histogram equalised image of TMI RTP VD1
			tmirtpvd1_raingomp.jpg	rain-gomp histogram equalised image of TMI RTP VD1
		rad	kthu_tenary.jpg	histogram equalised image with potassium-red, thorium-green and uranium-blue
			dose_enhanced.jpg	rain-gomp histogram equalised image of the dose rate with a NE gradient
			k_enhanced.jpg	rain-gomp histogram equalised image of equivalent concentration of potassium with a NE gradient
			th_enhanced.jpg	rain-gomp histogram equalised image of equivalent concentration of thorium with a NE gradient
			u_enhanced.jpg	rain-gomp histogram equalised image of equivalent concentration of uranium count with a NE gradient
GRAVITY	point_data		billabong_grav.dat	point located gravity survey station data (see readme.txt for details)
	grids		billabong_grav_2km.ers	2 km grid of gravity data
	images		grav_enhanced.jpg	pseudocolour histogram equalised image of gravity data with a NE gradient
			regional_grav_enhanced.jpg	pseudocolour histogram equalised image of regional gravity data with a NE gradient
	shapefiles		billabong_grav_stations.shp	locations of gravity survey stations